

NONUNIFORMLY SPACED LINEAR ARRAY DESIGN FOR THE SPECIFIED BEAMWIDTH/SIDELOBE LEVEL OR SPECIFIED DIRECTIVITY/SIDELOBE LEVEL WITH COUPLING CONSIDERATIONS

H. Oraizi and M. Fallahpour

Department of Electrical Engineering
Iran University of Science and Technology (IUST)
Narmak, Tehran, Iran

Abstract—In this paper, we investigate nonuniformly spaced linear arrays (NUSLA) rigorously. Several important problems in NUSLA design are solved with the combination of the Genetic Algorithm and Conjugate Gradient method (GA-CG). The pattern synthesis for the specified beamwidth and minimum achievable sidelobe level (SLL) are performed and for the first time, the graphs which show the relation between the beamwidth, sidelobe level and number of elements for NUSLA are derived. Also, the NUSLA's pattern for the specified directivity and sidelobe level is synthesized. The graphs showing the behavior of NUSLA relative to the increase of its length for a fixed number of elements are derived. These graphs show the relations between the directivity and sidelobe level of NUSLA with its length. As a practical design, an array of parallel dipoles is designed for specified beamwidth/sidelobe level or specified directivity/sidelobe level. Furthermore, a novel Neural Network based model for the NUSLA is presented for the rapid and accurate computation of S -parameters. The computed S -parameters are used for the computation of coupling among elements. Then the GA-CG method can adjust these values in the synthesis process to achieve desired pattern and bearable coupling among elements.

1. INTRODUCTION

The analysis of nonuniformly spaced linear arrays originated with the work of Unz [1], who developed a matrix formulation to obtain the current distribution necessary to generate a prescribed radiation pattern for a NUSLA with specified geometry. Subsequent to the initial

concept of Unz, NUSLA is divided into two categories: thinned arrays, which are derived by selectively zeroing some elements of an initial equally spaced linear array (ESLA), and arrays with randomly spaced elements.

In the first category, Skolnik [2] employed dynamic programming for zeroing elements. Mailloux and Cohen [3] utilized the statistical thinning of arrays with quantized element weights to improve side lobe level performance. The Genetic Algorithm [4–6] and Simulated Annealing (SA) [7] were used to thin an array. Razavi and Forooghi [8] used pattern search algorithm for array thinning.

In the second category that is of interest in this paper, Harrington [9] developed an iterative method to reduce the sidelobe levels of uniformly excited N -elements linear arrays by employing unequal spacing. His method can reduce the sidelobe level to about $2/N$ times the field intensity of the mainlobe without increasing the beamwidth of the mainbeam as obtained by ESLA. Andreasen [10] derived two important conclusions for NUSLA: 1) the 3-dB beamwidth of the mainlobe depends primarily on the length of the array and 2) the sidelobe level depends primarily on the number of elements in the array and to a minimal extent on the average element spacing of the array when the latter exceeds about two wavelengths. One of the first analytical methods in this category is Ishimaru's classical analysis [11] of NUSLA. His work addressed the following points: 1) sidelobe level reduction relative to a linear array with uniform excitation, 2) grating lobe suppression of the linear array by the use of the Anger function and 3) azimuthal frequency scanning by means of an unequally spaced circular array. In recent years, other works such as [12, 13] proposed an analytical method for nonuniformly spaced array synthesis.

As mentioned in [14], since the element positions occur as trigonometric or exponential functions, element position synthesis is a nonlinear problem. Also, element spacing constraints has to be placed on the solutions, for instance they must be real and positive and greater than prescribed value to reduce the array element count. Reference [15] determined element excitations required to yield desired field pattern for an array with arbitrary geometry. In [16], the particle swarm optimization is applied to the optimization of nonuniformly spaced antenna arrays and sidelobe level is reduced. In [17], with Neural Network (NN) and in [18] with least mean square, nonuniformly spaced array are synthesized.

Most works consider the minimization of the sidelobe level at a fixed main beamwidth and all of them consider the design problem as a single objective minimization problem. But there are no design curves which show minimum achievable SLL for a specified beamwidth

for NUSLA with N elements. Also, no work has been reported for the design of NUSLA with specified directivity and sidelobe level. Although, [19] provided directivity versus element spacing curves for ESLA with uniform excitation, there is no similar curves for NUSLA. Furthermore, the dependence of array directivity on its length and average element spacing for NUSLA is rarely addressed in the literature.

On the other hand, the mutual coupling (MC) consideration for NUSLA is a cumbersome work. In a few recent works [20, 21], driving point impedance matching has been derived with unequal spacing of elements. In [22], a NN-based model was developed to replace the induced EMF formulation for approximating the mutual coupling among array elements. This model has the notable advantage that it is not element specific. Reference [23] extends the array design developments reported in [20–22] to include the effects of frequency variation in the optimization process. The NN model in this work enabled rapid and accurate array element driving point impedance estimation as a function of frequency, element position and scan angle.

In the aforementioned studies, the MC is included in the driving point impedance. But according to [24], the coupling between two elements can be measured by an appropriate criterion, which may be defined for the transmitter and receiver individually. But this parameter has not been included in the NUSLA design. The main reason is the difficulty of its computation which requires S -parameters.

In this paper, we design NUSLA with N elements for the specified beamwidth between first nulls (BW) and minimum possible SLL . Then, for the first time a family of curves showing the relations among SLL , number of elements and beamwidth as parameter are derived with an optimization method. Also, NUSLA pattern synthesis for the specified directivity (D) and minimum achievable SLL is performed and average element spacing is defined. A curve for the directivity and SLL versus average element spacing is derived. Furthermore, an optimum dipole array for the specified D/SLL and specified BW/SLL with unequal spacing is designed. For the first time, we include coupling definition in [24] for the NUSLA design. We design NUSLAs for minimum (bearable) coupling or specified coupling between its adjacent elements. For the coupling calculation, a NN-based model which is not element specific is introduced and used to estimate S -parameters.

The combination of GA and Conjugate Gradient (CG) is used as the optimization method and the Neural Network is employed for the coupling computations (GA-CG-NN).

2. BASIC RELATIONS FOR NONUNIFORMLY SPACED LINEAR ARRAY DESIGN

The far field pattern of a NUSLA consisting of N elements placed at d_n as shown in Fig. 1 with uniform excitation is:

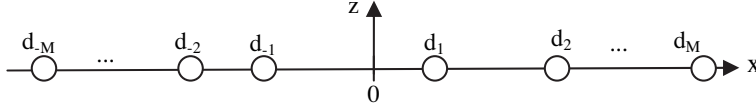


Figure 1. Nonuniformly spaced elements geometry.

$$E(\varphi) = \frac{1}{N} \sum_{n=-M}^{n=M} e^{jkd_n \cos \varphi} ; N = 2M + 1 \quad (1)$$

$$E(\varphi) = \frac{1}{N} \sum_{n=-M, n \neq 0}^{n=M} e^{jkd_n \cos \varphi} ; N = 2M \quad (2)$$

And for symmetrical geometry around origin:

$$E(\varphi) = \frac{1}{N} \left[1 + \sum_{n=1}^{n=M} \cos(kd_n \cos \varphi) \right] ; N = 2M + 1 \quad (3)$$

$$E(\varphi) = \frac{1}{N} \sum_{n=1}^{n=M} \cos(kd_n \cos \varphi) ; N = 2M \quad (4)$$

where k is the wave number and φ and θ are the angle from the array axis (x axis) and the z axis, respectively. Because of symmetry, only $\theta = 90$ degree plane pattern is sufficient. Thus, φ is used as the angle from the array axis in the $\theta = 90$ degree plane.

The sidelobe level is defined as:

$$SLL = \max(|E(\varphi)|) |_{\varphi \in \varphi_{sl}} \quad \varphi_{sl} = [0, \varphi_{FNL}] \cup [\varphi_{FNR}, 180] \quad (5)$$

where φ_{FNL} and φ_{FNR} are the left and right first nulls around the broadside mainbeam. For the symmetrically specified beamwidth BW (null-to-null) case, these values are known to be:

$$\varphi_{FNR} = 90 + \left| \frac{BW}{2} \right| , \quad \varphi_{FNL} = 90 - \left| \frac{BW}{2} \right| \quad (6)$$

Also for a specified SLL , the values of these nulls can be approximately assumed to be equal to the nulls of ESLA with the same SLL . Then the

Taylor formula [25], gives these nulls. Also we may use a null finding procedure to achieve the exact position of these nulls.

Another important parameter is directivity. A relation for the directivity of an array with isotropic elements is given in [19] as:

$$D = \frac{\left(\sum_{k=-M}^M I_k \right)^2}{\sum_{m=-M}^M \sum_{p=-M}^M I_m I_p e^{j(\alpha_m - \alpha_p)} \frac{\sin(k(d_m - d_p))}{k(d_m - d_p)}} \quad (7)$$

where I_n and α_n are amplitude and phase of n th element's excitation, respectively. In this paper, $I_n = 1$ and $\alpha_n = 0$. When isotropic elements are replaced with parallel dipoles an approximate relation for the whole array directivity (D_w) is obtained as:

$$D_w \approx D_e \cdot D \quad (8)$$

where D_e is the element directivity and D is directivity of the array factor (Eq. (7)). But this relation may not be sufficiently accurate and may cause unbearable error. Reference [21] derived an approximate formula for the directivity of a parallel half wavelength dipoles array (shown in Fig. 2) as:

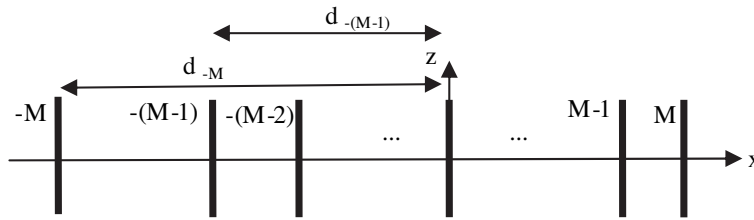


Figure 2. The position and orientation of dipoles in NUSLA.

$$D_w(\varphi) \cong \frac{\sum_{m=-M}^M \sum_{n=-M}^M I_m I_n e^{jk(d_m - d_n)(\cos \varphi - \cos \varphi_0)}}{\sum_{m=-M}^M \sum_{n=-M}^M I_m I_n e^{-jk(d_m - d_n)k \cos \varphi_0} \tilde{S}(k(d_m - d_n))} \quad (9)$$

where

$$\tilde{S}(x) = \frac{\pi}{16} \left[3J_0 \left(\frac{x}{2} \right) - 4J_1^2 \left(\frac{x}{2} \right) + J_2^2 \left(\frac{x}{2} \right) \right] \quad (10)$$

and

$$\tilde{S}(0) \cong 0.609412 \quad (11)$$

and mainbeam of the array is directed along $\theta = 90^\circ$ and $\varphi = \varphi_0$. If we select $\varphi_0 = 90^\circ$ and $I_n = 1$, then the maximum value of $D(\varphi)$ occurs at $\varphi = 90^\circ$. Eqs. (5), (7) and (9) show that SLL and D are nonlinear functions of element spacing d_n .

Also, for NUSLA, we define an average element spacing as:

$$d_{ave} = \frac{L}{N-1} \quad (12)$$

where L is the total length of the array, which for a uniform spacing d , is:

$$L = (N-1)d \quad (13)$$

This parameter also can be judged as an approximate criterion for the coupling. Greater d_{ave} , may lead to the reduction of MC.

3. NUSLA DESIGN FOR SPECIFIED BEAMWIDTH AND MINIMUM SIDELobe LEVEL (PENCIL BEAM)

In this section, with nonuniform spacing, for tightly specified beamwidth between first nulls (BW), the minimum achievable sidelobe level is derived. The NUSLA is designed to have minimum SLL for very tightly specified symmetrical beamwidth. In this section, the array geometry is assumed symmetric around the origin to reduce the unknown variables. Therefore, array pattern is symmetrical and right or left sides of mainbeam is similar to each other. First null is selected to be $\varphi_{FN} = \varphi_{FNR}$ and is calculated by Eq. (6). To solve this nonlinear problem, a fitness function (error function) is defined as:

$$\begin{aligned} error_{BW-SLL} &= error_{BW} + error_{SLL} \\ error_{BW} &= \begin{cases} 0 & \text{if } |E(\varphi_{FN})| \leq 0.001 \\ 10 & \text{else} \end{cases} \\ error_{SLL} &= \max(|E(\varphi)|) |_{\varphi \in \varphi_{sl}} \end{aligned} \quad (14)$$

Tightly specified beamwidth means that the first null has to be located exactly at φ_{FN} . Thus beamwidth error ($error_{BW}$) definition, should give a high error value (for example 10) when the first null deviates from this angle.

All variables to be calculated to minimize the fitness function are the M element positions. These variables are derived with the optimization algorithm.

In all of this paper we use a hybrid optimization algorithm. This algorithm is the combination of the Genetic Algorithm and Conjugate Gradient (GA-CG). Since GA as an evolutionary algorithm is supposed to be a global optimization method, it does not heavily depend on the initial values of the variables. However, implementation of GA is very computer time consuming. On the other hand, CG is largely a local optimization method and its convergence to an extremum point depends on the initial values of variables. However, implementation of CG is relatively fast, but it requires the computation of gradients of functions. Consequently, combination of GA and CG may utilize the advantages of each one, avoiding the shortcomings of both. Therefore, the combined algorithm starts by implementing GA with a set of initial values for variables which leads towards an extremum. At about this point, GA is stopped and CG is activated to speed up the convergence towards a local extremum. Thereafter, the values of variables at this extremum point are taken as the initial values for GA. This algorithm is continued until the global extremum is arrived at. In all optimizations, the element positions are assumed to be as $d_n = d_n^{(0)} + \delta d_n$. Where $d_n^{(0)}$ is an appropriate value for the n th element position and δd_n is its variation, which is calculated by the hybrid algorithm to meet the desired conditions. The complete flowchart of the GA-CG method is shown in Fig. 3.

To illustrate the efficacy of the proposed method, a broadside pencil beam with 16 degree symmetrical beamwidth is designed for NUSLA with 20 elements. For this case, $\varphi_{FN} = 98^\circ$. The values of $d_n^{(0)}$ are selected as the positions of elements in ESLA with 0.4λ spacings and the same number of elements. The hybrid algorithm finds optimum position of elements. The values of d_n are listed in Table 1 and minimum achievable SLL is -24.87 dB. Also the optimum designed NUSLA's pattern is shown in Fig. 4.

Table 1. Position of elements for optimum designed NUSLA ($N = 20$).

n	-10	-9	-8	-7	-6	-5	-4	-3	-2	-1
d_n / λ	-4.37	-3.597	-2.928	-2.449	-1.956	-1.614	-1.184	-0.85	-0.537	-0.104
n	1	2	3	4	5	6	7	8	9	10
d_n / λ	0.104	0.537	0.85	1.184	1.614	1.956	2.449	2.928	3.597	4.37

As it is clear from Fig. 4, the optimum NUSLA's pattern with uniform excitation is similar to the Dolph-Chebyshev pattern for equally spaced linear array with tapered excitation. Therefore, NUSLA

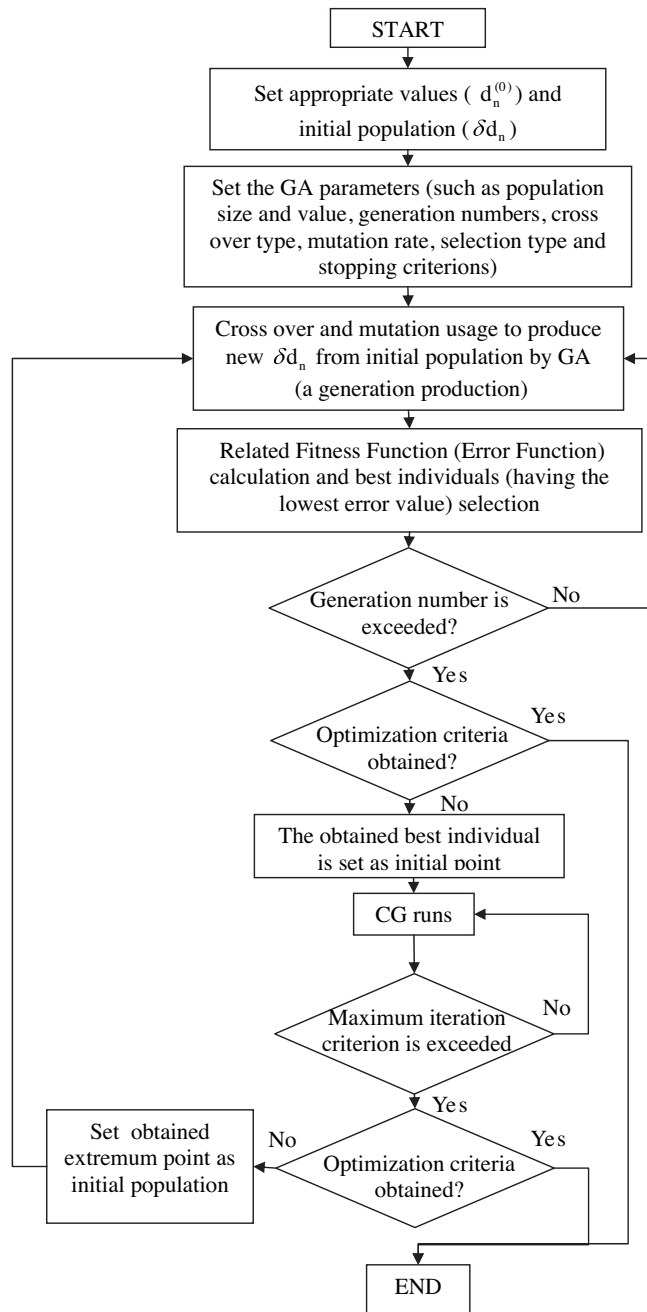


Figure 3. The complete flowchart of the GA-CG method.

with simple feed network can generate a pattern similar to the Dolph-Chebyshev pattern. Also, it is verified that the minimum SLL for a specified BW by the hybrid algorithm may be realized because the Dolph-Chebyshev pattern has the minimum SLL for a specified BW .

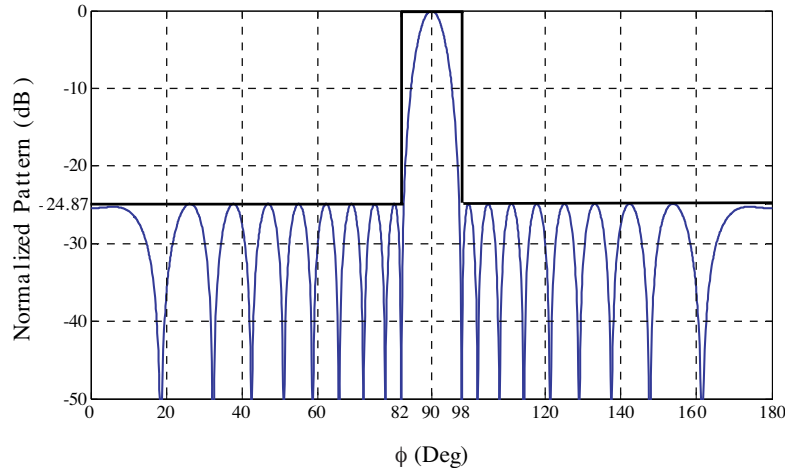


Figure 4. Pattern of designed NUSLA for $BW = 16^\circ$ and minimum achieved $SLL = -24.78$ dB.

Although for the equally spaced linear array with N elements and spacing d , the Dolph-Chebyshev excitation gives minimum SLL for a specified BW , but for nonuniformly spaced linear array, there is no similar relation for the element spacing. In fact, the main reason is due to the nonlinear relation between d_n and $E(\varphi)$. Here, for the first time, with the hybrid algorithm, for a specified BW and constant N , the minimum SLL is achieved for NUSLA. The results for $N = 8, 10, 12, 14, 16, 18, 20, 30$ and $BW = 8, 12, 16, 20$ degrees are drawn in Fig. 5.

As Fig. 5 shows, the minimum SLL for constant N and specified BW is a function of both the number of elements (N) and BW . Furthermore, for a narrow BW and small N , low SLL is not realizable. A narrow BW pattern requires longer array length. Therefore, for small N , very wide element spacing between two adjacent element becomes necessary and a secondary mainbeam (equivalent to grating lobe in ESLA) appears. Consequently, low SLL for small N , is impossible to obtain because of these conflicting requirements.

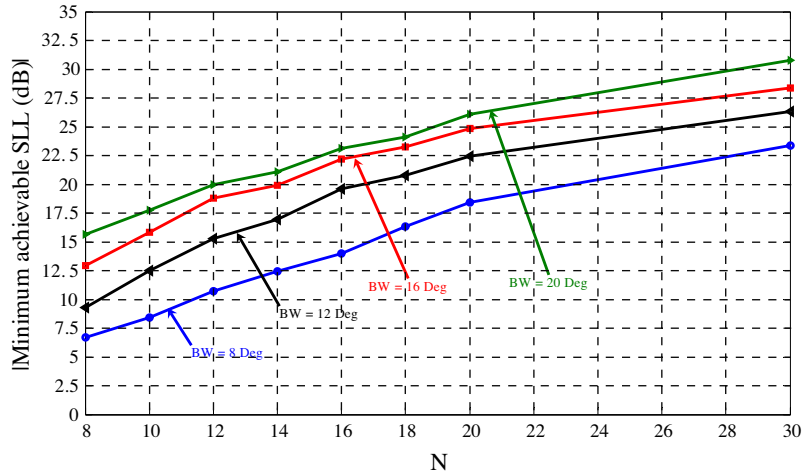


Figure 5. (Minimum achievable SLL)- N curves with BW as parameter for NUSLA.

4. NUSLA DESIGN FOR SPECIFIED DIRECTIVITY AND SIDELobe LEVEL

In Section 3, we designed for the minimum SLL and tightly specified beamwidth. However, sometimes designers may desire to design NUSLA for a specified directivity. The narrowest beamwidth may be judged as maximum directivity, but it is not always the case. When the array length of equally spaced linear array with mainbeam in φ_0 direction, increases (for constant N), beamwidth decreases and directivity increases until the element spacing (d) exceeds $\lambda/(1 + |\cos \varphi_0|)$ and grating lobe appears [19]. With the grating lobe appearance, the beamwidth still decreases but directivity falls so rapidly that the inverse relation between D and beamwidth is not true in this condition. For the broadside pattern ($\varphi_0 = 90^\circ$), when d exceeds 1λ , this situation happens. But what happens for the nonuniformly spaced linear array in a similar condition? Before answering this question, we would like to show that the NUSLA design for a constant specified BW should not be interpreted as NUSLA design for constant D .

4.1. Directivity and Beamwidth Relationship

To show the relationship between directivity and BW for the designed NUSLA in Section 3 which its results is shown in Fig. 5, directivity is

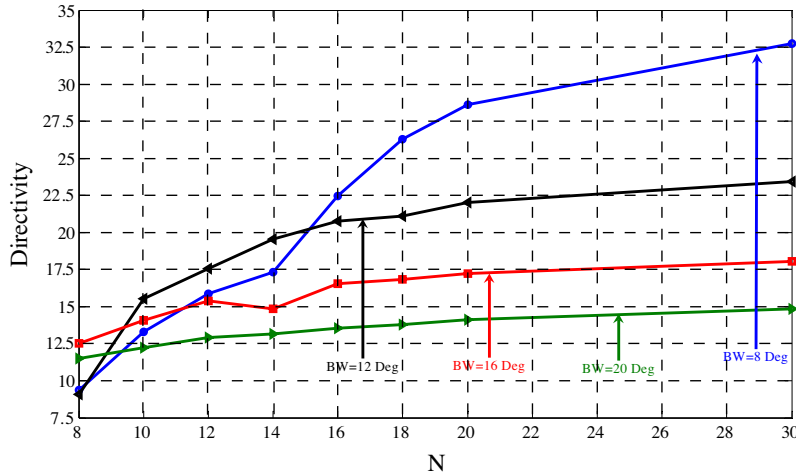


Figure 6. Directivity- N curves with BW as parameter for the designed NUSLA in Section 3 for the minimum SLL and tightly specified BW .

calculated by Eq. (7) and plotted in Fig. 6. In this figure, D is drawn versus N and BW is a parameter. As we expect, the directivity for a pattern with constant BW , is not constant and changes with N and spacing. Also, for instance, for $BW = 8^\circ$, when N is smaller than 16, the array directivity becomes smaller than the directivity of array with the same number of elements but $BW = 12^\circ$. These results show that in the case of array pattern design for a specified directivity, sometimes BW is not a good criterion.

Therefore, we propose the hybrid algorithm to design NUSLA with the specified D and bearable SLL .

Fitness function (error function) for this problem defined as:

$$\begin{aligned}
 error_{D-SLL} &= error_D + error_{SLL} \\
 error_D &= |D - D_{desired}|^2 \\
 error_{SLL} &= \begin{cases} |SLL(\text{dB}) - SLL_{threshold}(\text{dB})|^2 & \text{if } SLL(\text{dB}) > SLL_{threshold}(\text{dB}) \\ 0 & \text{else} \end{cases}
 \end{aligned} \tag{15}$$

where $D_{desired}$ is the desired directivity and $SLL_{threshold}$ is the bearable SLL in dB.

For example we design NUSLA with $N = 14$, $D_{desired} = 22$ for $SLL_{threshold} = -15$ dB. Also, a Minimum Allowable Distance (MAD) between two adjacent elements is included to reduce mutual coupling.

Then, the hybrid algorithm should solve the problem with the MAD constraint according to:

$$|d_n - d_{n\pm 1}| > MAD \quad (16)$$

Here, we set $MAD = 0.5\lambda$. The hybrid algorithm solved this problem. The resultant directivity is 22.1 and SLL is -15.5 dB. The values of d_n are listed in Table 2. Because of symmetry, only positions of right side elements are listed. Also, the optimally designed NUSLA's pattern is shown in Fig. 7.

Table 2. Position of right side elements for optimum designed NUSLA ($N = 14$).

n	1	2	3	4	5	6	7
d_n / λ	0.31	1.1	1.92	2.92	3.72	4.74	5.56

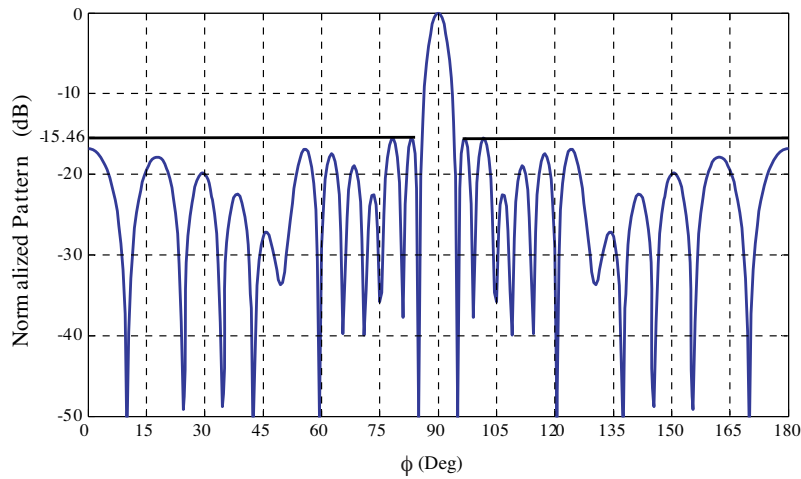


Figure 7. Pattern of designed NUSLA ($N = 14$) with $D = 22.1$ and $SLL = -15.46$ dB.

In second example, we design a NUSLA with $N = 20$, $D_{desired} = 20$ and $SLL_{threshold} = -21$ dB. Here, $MAD = 0.35\lambda$ is assumed. The hybrid algorithm solved this problem. The resultant directivity is 20 and SLL is -22.6 dB. The values of d_n are listed in Table 3. Because of symmetry, only position of right side elements are listed. Also, the optimally designed NUSLA's pattern is shown in Fig. 8.

Table 3. Position of right side elements for optimum designed NUSLA ($N = 20$).

n	1	2	3	4	5	6	7	8	9	10
d_n/λ	0.2	0.58	1.03	1.43	1.85	2.37	2.87	3.47	4.26	5.06

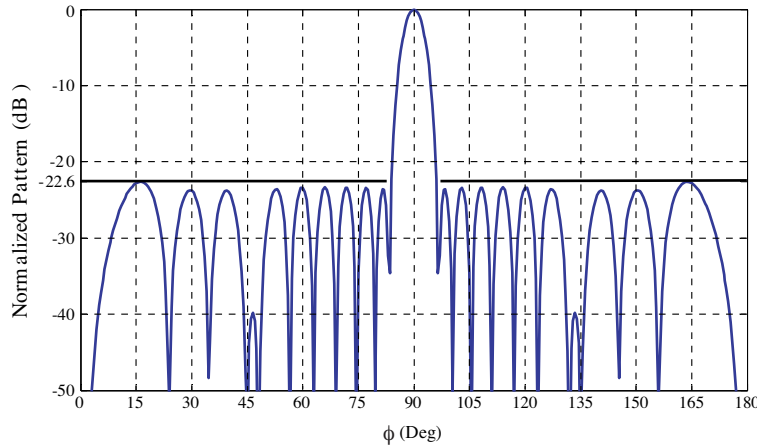


Figure 8. Pattern of designed NUSLA ($N = 20$) with $D = 20$ and $SLL = -22.6$ dB.

It is necessary to mention that, there is a trade-off between D and SLL . Whenever the desired D is high, a low SLL is difficult to obtain.

We can enhance the value of directivity error or SLL error in Eq. (15) by weighting functions as follow:

$$error_{D-SLL} = W_D error_D + W_{SLL} error_{SLL} \tag{17}$$

where, W_D and W_{SLL} are the weights for directivity and SLL , respectively.

Therefore, with proper weighting, Eq. (17) may be used to design NUSLA for a desired D and bearable SLL or a desired SLL and threshold D .

4.2. Directivity and Length Relationship for NUSLA

To answer the question about NUSLA’s directivity behavior when for a fixed number of elements, the array length increases, average element spacing defined in Eq. (12), should be used. For the fixed number of elements which is assumed 11, the array length slightly become longer,

and d_{ave} from Eq. (12) becomes wider. And then for each new length (or new d_{ave}), with the hybrid algorithm, the optimum NUSLA is designed to show a suitable directivity in comparison with ESLA with the same length and same number of elements.

Here, with the hybrid algorithm, for some d_{ave} , NUSLA is designed to satisfy some constraints as follows:

1. The whole length of NUSLA should be exactly equal to the specified value $((N - 1)d_{ave})$ as:

$$|d_M - d_{-M}| = (N - 1)d_{ave} \quad (18)$$

2. For $d_{ave}/\lambda \leq 0.5$, $MAD = d_{ave}$ and for $d_{ave}/\lambda > 0.5$, $MAD = 0.5\lambda$.

The desired directivity is specified to be as ESLA's directivity ($D_{uniform}$) for $d_{ave}/\lambda \leq 0.9$ and bearable SLL equal to -13 dB. But for $d_{ave}/\lambda > 0.9$, that the grating lobe appears for ESLA and directivity falls rapidly, the NUSLA design purpose is reasonable SLL and maximum achievable directivity. Therefore, Eq. (17) with suitable W_D and W_{SLL} can be used as a fitness function. The elements of NUSLA are not necessary to be symmetrically located. Therefore, Eqs. (1) or (2) for $E(\varphi)$ may be used. The hybrid algorithm found optimum NUSLA for some d_{ave} and $N = 11$. Their D and SLL are plotted in Figs. 9 and 10, respectively. Also, in these figures, the directivity and SLL of ESLA for element spacing d_{ave} and $N = 11$ are also shown. These results show that NUSLA for $1.4 > d_{ave}/\lambda > 0.9$ still results in good directivity and reasonable SLL .

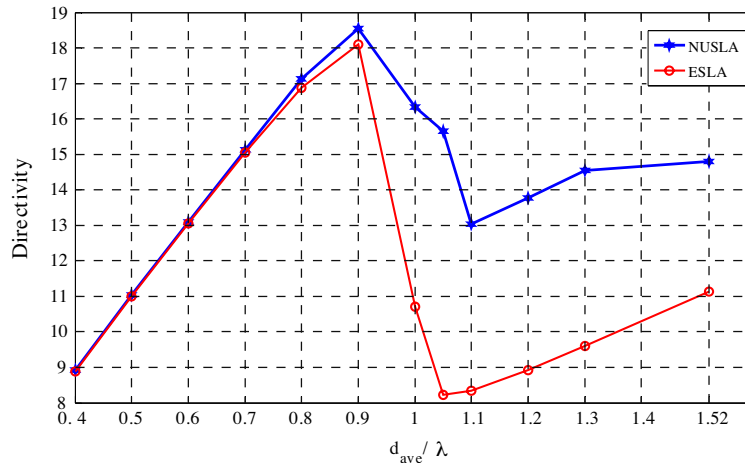


Figure 9. Comparison of D of ESLA and NUSLA having the same average element spacing for $N = 11$.

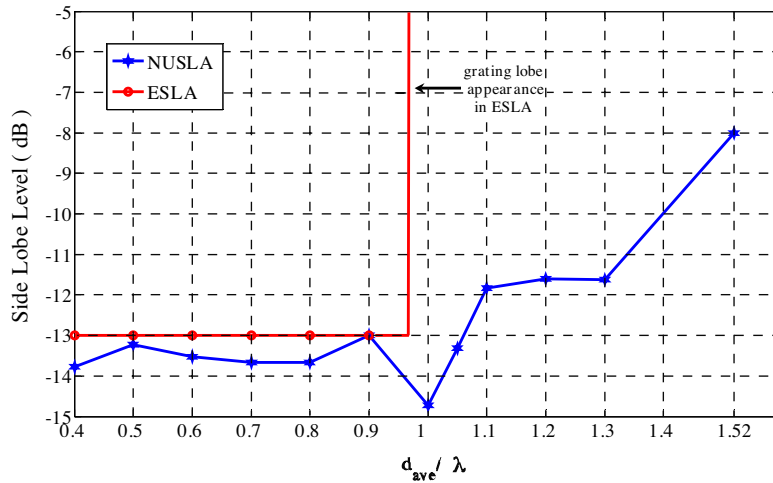


Figure 10. Comparison of *SLL* of ESLA and NUSLA having the same average element spacing for $N = 11$.

The pattern of optimum NUSLA for $d_{ave} = 1.2\lambda$ and that of ESLA with the spacing $d_{ave} = 1.2\lambda$ between its elements is shown in Fig. 11. The element positions for NUSLA and ESLA are also shown in Fig. 12. As we can see, the minimum distance between elements is 0.68λ and maximum distance is 2.77λ to ensure the reduction of MC among elements.

5. NONUNIFORMLY SPACED PARALLEL DIPOLE ARRAY DESIGN

In this section, with the obtained results in Sections 3 and 4, the NUSLA with dipole elements will be designed.

5.1. Dipole Array Design for Specified *BW* and Minimum Achievable *SLL*

Consider an array of half wavelength dipoles with $N = 16$ as shown in Fig. 2. It is desired to have $BW = 12^\circ$ with $MAD = 0.5\lambda$. With reference to Fig. 5, it is found that minimum achievable *SLL* is about -19.5 dB. The optimum position of elements for this case, which was calculated by the hybrid algorithm, is listed in Table 4. Because of symmetry only the positions of right side elements are listed.

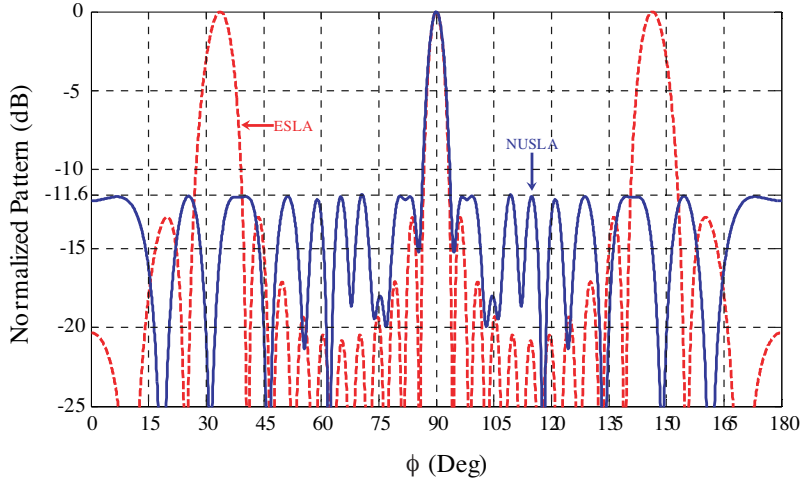


Figure 11. Comparison of radiation pattern of ESLA and NUSLA for $d_{ave} = 1.2\lambda$ and $N = 11$.

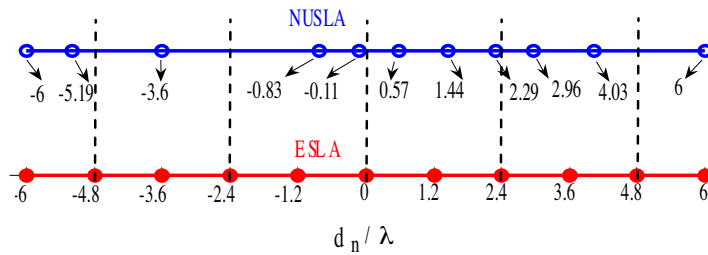


Figure 12. Comparison of element positions in ESLA and NUSLA for $d_{ave} = 1.2\lambda$ and $N = 11$.

Table 4. Positions of right side elements for optimum designed parallel dipole array ($N = 16$).

n	1	2	3	4	5	6	7	8
d_n / λ	0.252	0.793	1.436	1.992	2.616	3.44	4.272	5.134

The whole array pattern (E_w) is defined as:

$$E_w = E \cdot E_e \quad (19)$$

where E is the array factor (array with isotropic elements) defined in Eqs. (1), (2), (3) and (4) and E_e is the element pattern of the half

wavelength dipole shown in Fig. 2, defined as:

$$E_e = \cos\left(\frac{\pi}{2} \cos \theta\right) / \sin \theta \tag{20}$$

The whole pattern of the designed parallel dipole array is drawn in the horizontal plane ($\theta = 90^\circ$) in Fig. 13. As we expected, the element pattern does not change the first null position and *SLL* from those of the array factor.

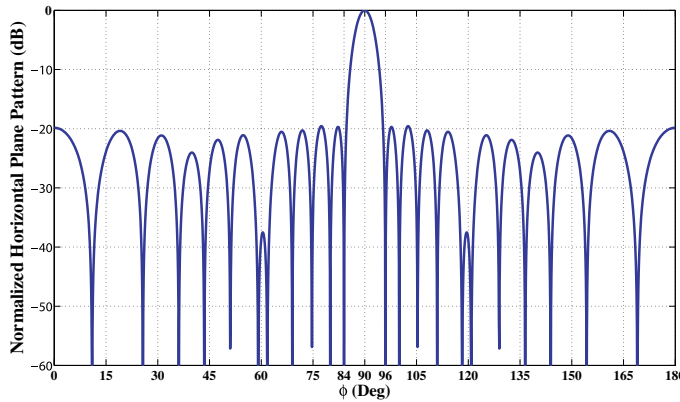


Figure 13. The horizontal plane pattern of the designed parallel dipole array ($N = 16$, $BW = 12^\circ$).

5.2. Dipole Array Design for Specified Directivity and *SLL*

Consider the dipole array in Section 5.1 with $N = 12$. It is desired to have a pattern with $D_w = 25$ (13.98 dBi) and minimum achievable *SLL* with $SLL_{threshold} = -17$ dB for $MAD = 0.55\lambda$.

We use the result of Section 4 and Eq. (8) to design the array factor with desired directivity. For half wavelength dipoles, $D_e = 1.64$.

Table 5. Position of right side elements for optimum designed parallel dipole array ($N = 12$).

n	1	2	3	4	5	6
d_n / λ	0.28	0.84	1.41	2.09	2.88	3.69

The Eq. (8) gives $D = D_w/D_e = 25/1.64 = 15.24$, then with this desired directivity and Eq. (15), the hybrid algorithm will find the optimum d_n for symmetrical geometry. Because of symmetry only the right side element positions are listed in Table 5. The achieved D is 15.5 and $SLL = -18.52$ dB. The whole directivity is 25.42 (14.05 dBi). The whole directivity in the horizontal plane is drawn in Fig. 14.

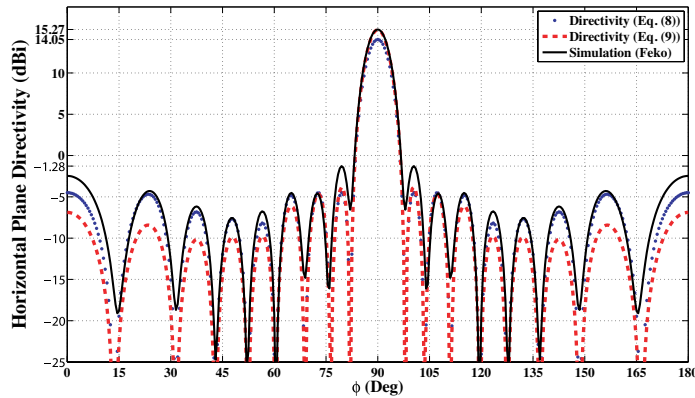


Figure 14. The directivity of the designed parallel dipole array, calculated by Eq. (8), Eq. (9) and simulation.

This array is simulated by fullwave software, FEKO program [26]. For excitation, voltage sources with input impedances of 125 ohm are used. The directivity of simulated array in the horizontal plane is drawn in Fig. 14. As we can see, for the peak directivity at $\varphi = 90^\circ$, there is 1.22 dBi difference between simulation and design values. This difference is due to the fact that Eq. (8) is an approximate formula. But it is acceptable. Also to show the accuracy of Eq. (9), in comparison with Eq. (8), the directivity of the designed array, is calculated by Eq. (9) and plotted in Fig. 14. There is a good agreement between its results and simulation results. In Section 5.3, Eq. (9) will be used for the array design. It should be mentioned that MC causes the first sidelobe in the simulation results to become greater than our design value.

5.3. Dipole Array Design for Bearable Coupling Between Adjacent Elements

In Section 5.2, the nonuniformly spaced dipole array was designed for the specified D and SLL with some constraints on element positions. The average element spacing and MAD were introduced in this paper

as some criteria to limit coupling among elements. But these criteria are not accurate enough. In [27–29], MC is defined. The coupling between two transmitter antennas is defined in [24] as:

$$C_{21} = \frac{P_2}{P_1} = \frac{|S_{21}|^2}{1 - |S_{11}|^2} \quad (21)$$

where P_2 is the power received by antenna 2 and P_1 is the power delivered by antenna 1. This parameter is a better criterion than MAD or d_{ave} . However, for NUSLA, the S -parameters computation for various distances among elements is a very cumbersome and time consuming problem. Since the array geometry is not kept fixed in the optimization process, the S -parameters should be computed in each run of GA-CG. On the other hand, the S -parameters computation is very difficult and their relations are scarce and imprecise. The array simulation by a fullwave simulator like IE3D is the best procedure, but by using the simulator for data generation for GA-CG, the CPU time may increase abruptly. To overcome this problem, we propose a NN-based model for the S -parameters estimation. Although NN is used for solving some various antenna problems [30–33], NN using for the calculation of S -parameters is proposed for the first time.

We propose a Radial Basis Function Neural Network (RBFNN) with three layers. For the training stage, we should generate the data with a fullwave simulator like IE3D. As a good approximation, only the adjacent element effects are included in the simulation. Since the maximum coupling occurs between two neighboring elements, we consider an array of three half wavelength dipoles with variable element spacing d_1 and d_2 as shown in Fig. 15 and simulate it by IE3D at 3 GHz. Computed S -parameters are used for RBFNN training. The values of d_1 and d_2 are selected from the set{10, 20, 30, 40, 50, 60, 70, 80, 90, 100, 110, 120, 130, 160, 200} all in mm. For instance, one possible case for (d_1, d_2) is (40 mm, 50 mm). About $15 \times 15 = 225$ simulations are performed and S -parameters are obtained to train RBFNN. After the training and testing, RBFNN may be used to estimate S -parameters between each two adjacent elements of NUSLA for element spacing from [10–200] all in millimeter with 0.1 mm precision. In order to implement the proposed RBFNN model, the Neural Networks Toolbox of MATLAB, is used. The main properties of the RBFNN of this toolbox are the utilization of Gaussian distribution transfer functions in the hidden layer, pure linear transfer functions in the output layer, and the least mean squares algorithm for training in the output layer and optimization of weights between neurons. For the hidden layer, the center of Gaussian distribution transfer functions is calculated by k-means algorithm. The

trained RBFNN has 255 neurons in the hidden layer and 6 neurons in output layer (real and imaginary parts of S-parameters are separately produced by RBFNN). This NN-based model is used by the hybrid optimization method. For instance, when the optimizer is to calculate C_{24} and C_{34} , it gives ($d_{24} = |d_2 - d_4|$, $d_{34} = |d_3 - d_4|$) to RBFNN which generates S_{44} , S_{24} and S_{34} and then C_{24} and C_{34} by Eq. (21) can be computed. Block diagram in Fig. 16 shows the proposed process.

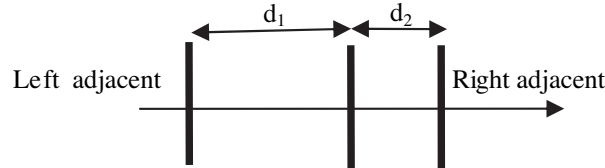


Figure 15. Three half wavelength dipoles with variable element spacing d_1 and d_2 .

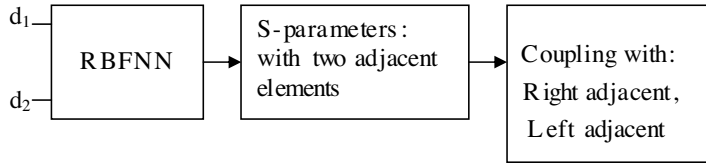


Figure 16. S-parameters estimation by NN and computation of coupling with two adjacent elements.

Table 6. The optimum position of right side dipoles d_n/λ obtained by GA-CG-NN.

n	1	2	3	4	5	6	7	8
d_n/λ	0.26	0.74	1.25	1.73	2.25	2.75	3.35	4.28

Now, we can design NUSLA for a specified C_{ij} between two adjacent elements. The fitness function (error function) is defined as:

$$error_{D-SLL-C} = W_D error_D + W_{SLL} error_{SLL} + W_C error_C \quad (22)$$

The first two terms on the right side are the same as Eq. (17) and $error_C$ shows the deviation from the bearable coupling and may be defined in various forms. W_C is an enhancing coefficient, like W_D and W_{SLL} .

Here, for parallel half wavelength dipole array with $N = 16$, it is desired to have $SLL = -16$ dB. Also, D is to be greater than 30 and $|\max(C_{ij})| > 29$ dB.

With these conditions, the optimization with GA-CG-NN method is performed. For the directivity computation, Eq. (9) which is accurate sufficiently was used. The optimum position of right side elements is listed in Table 6 and C_{ij} are listed in Table 7. The achieved peak directivity is 36.4 or 15.61 dBi and achieved SLL is -16.92 dB. Also, $|\max(C_{ij})| = 29.4$ is achieved. The directivity in the $\theta = 90^\circ$ plane (horizontal plane) is shown in Fig. 17.

This array is simulated by FEKO for $f = 3$ GHz with unit voltage sources with 125 ohm impedances as excitations. The simulation directivity in the horizontal plane is shown in Fig. 17. The peak directivity is $D = 15.61$ dBi or $D = 36.4$. The values of C_{ij} derived from S -parameters by IE3D, are listed in Table 7 and compared with NN results. The value of SLL is -16.5 dB. As we expected, by keeping coupling among elements below a specified bearable value, its effect decreases. This is clearly seen by comparing Fig. 14 and Fig. 17 especially in the first sidelobe and mainbeam. The data reported in Table 7 verify the accuracy of the used RBFNN model for the calculation of S -parameters and then C_{ij} .

Table 7. Coupling in dB between each two adjacent elements of the optimized dipole array which is computed by NN model and IE3D.

n	$C_{n,n-1}$ (dB) (NN)	$C_{n,n-1}$ (dB) (Simulation)	$C_{n,n+1}$ (dB)(NN)	$C_{n,n+1}$ (dB)(Simulation)
-7	-38.8156	-39.2257	-29.5123	-31.6374
-6	-31.3448	-31.9237	-29.4018	-31.7746
-5	-29.8641	-31.8301	-30.0084	-31.9677
-4	-29.7291	-31.9356	-29.5219	-32.0627
-3	-29.4741	-32.0658	-29.5617	-31.8354
-2	-29.5741	-31.8354	-29.4556	-32.1938
-1	-29.5386	-32.2047	-29.7186	-31.9496
1	-29.7291	-31.9496	-29.5219	-32.2047
2	-29.4741	-32.1938	-29.5617	-31.8354
3	-29.5741	-31.8354	-29.4556	-32.0658
4	-29.5386	-32.0627	-29.7186	-31.9356
5	-30.0176	-31.9677	-29.8533	-31.8301
6	-29.3907	-31.7746	-31.3384	-31.9237
7	-29.4981	-31.6374	-38.8571	-39.2257

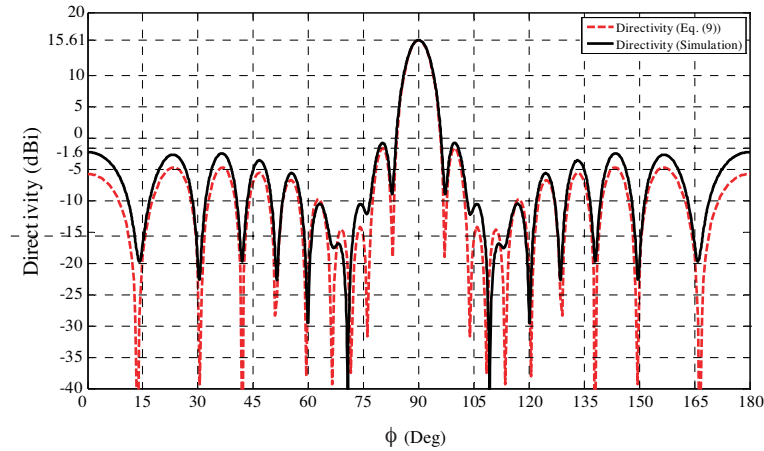


Figure 17. Directivity of optimized NUSLA in the horizontal plane ($\theta = 90^\circ$) from Eq. (9) and simulation in FEKO.

6. CONCLUSION

In this paper, nonuniformly spaced linear array was investigated rigorously. By the combination of GA-CG as an optimizer, some important problems were solved for this type of arrays. For the first time the relation between *SLL-BW* and number of elements for NUSLA were derived and plotted in the design curves. The NUSLA was designed for fixed N and BW to have minimum possible *SLL*. Also, for the first time, directivity was included in NUSLA design and NUSLA was optimally designed for specified directivity to have bearable (threshold) *SLL*. By using average element spacing, the relation between array length, directivity and *SLL* was derived for NUSLA and compared with ESLA with uniform excitation. As a result, NUSLA for wider average element spacing (e.g., wider than 1λ), still had a good performance whereas ESLA's performance degrade badly for such element spacing. As a practical design, parallel half wavelength dipole array was designed for specified BW and minimum achievable *SLL* using the results of arrays of isotropic elements. Then this array was designed for specified directivity and *SLL* with some constraint on the minimum distance among elements. For directivity computation, multiplication of array factor directivity and element directivity was used with good accurate results. The dipole array was designed for specified directivity and *SLL* and a novel constraint, bearable coupling among elements. Here, Neural Network model was used for the calculation of *S*-parameters and coupling among elements.

The obtained results show the efficacy of the hybrid algorithm. These results are general and may be used for nonuniformly spaced linear array with arbitrary elements.

ACKNOWLEDGMENT

This work is supported in part by Iran Telecommunication Research Center (ITRC).

REFERENCES

1. Unz, H., "Linear arrays with arbitrarily distributed elements," *IRE Trans. Antennas Propagat.*, Vol. 8, 222–223, Mar. 1960.
2. Skolnik, M. I., J. W. Sherman III, and G. Nemhauser, "Dynamic programming applied to unequally spaced arrays," *IEEE Trans. Antennas Propagat.*, Vol. 12, 35–43, Jan. 1964.
3. Mailloux, R. J. and E. Cohen, "Statistically thinned arrays with quantized element weights," *IEEE Trans. Antennas Propagat.*, Vol. 39, 436–447, Apr. 1991.
4. Haupt, R. L., "Thinned arrays using genetic algorithms," *IEEE Trans. Antennas Propagat.*, Vol. 42, No. 7, 993–999, July 1994.
5. Donelli, M., S. Caorsi, and F. DeNatale, M. Pastorino, and A. Massa, "Linear antenna synthesis with a hybrid genetic algorithm," *Progress In Electromagnetics Research*, PIER 49, 1–22, 2004.
6. Mahanti, G. K., N. Pathak, and P. Mahanti, "Synthesis of thinned linear antenna arrays with fixed sidelobe level using real coded genetic algorithm," *Progress In Electromagnetics Research*, PIER 75, 319–328, 2007.
7. Meijer, C. A., "Simulated annealing in the design of thinned arrays having low sidelobe levels," *Proc. South African Symp. Communication and Signal Processing*, 361–366, 1998.
8. Razavi, C. A. and K. Forooraghi, "Thinned arrays using pattern search algorithms," *Progress In Electromagnetics Research*, PIER 78, 61–71, 2008.
9. Harrington, R. F., "Sidelobe reduction by nonuniform element spacing," *IRE Trans. Antennas Propagat.*, Vol. 9, 187, Mar. 1961.
10. Andreasan, M. G., "Linear arrays with variable interelement spacings," *IEEE Trans. Antennas Propagat.*, Vol. 10, 137–143, Mar. 1962.

11. Ishimaru, A., "Theory of unequally-spaced arrays," *IRE Trans. Antennas Propagat.*, Vol. 10, 691–702, Nov. 1962.
12. Kumar, B. P. and G. R. Branner, "Design of unequally spaced arrays for performance improvement," *IEEE Trans. Antennas Propagat.*, Vol. 47, No. 3, 511–523, Mar. 1999.
13. Kumar, B. P. and G. R. Branner, "Generalized analytical technique for the synthesis of unequally spaced arrays with linear, planar, cylindrical or spherical geometry," *IEEE Trans. Antennas Propagat.*, Vol. 53, No. 2, 621–634, Feb. 2005.
14. Chen, K., Z. He, and C. Han, "A modified real GA for the sparse lineararray synthesis with multiple constraints," *IEEE Trans. Antennas Propagat.*, Vol. 54, No. 7, 2169–2173, July 2006.
15. Zhang, Y. F. and W. Cao, "Array pattern synthesis based on weighted biorthogonal modes," *J. of Electromagn. Waves and Appl.*, Vol. 20, No. 10, 1367–1376, 2006.
16. Lee, K.-C. and J.-Y. Jhang, "Application of particle swarm algorithm to the optimization of unequally spaced antenna arrays," *J. of Electromagn. Waves and Appl.*, Vol. 20, No. 14, 2001–2012, 2006.
17. Ayestarán, R. G., F. Las-Heras, and J. A. Martínez, "Non uniform-antenna array synthesis using neural networks," *J. of Electromagn. Waves and Appl.*, Vol. 21, No. 8, 1001–1011, 2007.
18. Kazemi, S. and H. R. Hassani, "Performance improvement in amplitude synthesis of unequally spaced array using least mean square method," *Progress In Electromagnetics Research B*, Vol. 1, 135–145, 2008.
19. Stutzman, L. and G. A. Thiele, *Antenna Theory and Design*, 120–121, John Wiley & Sons, 1998.
20. Bray, M. G., D. H. Werner, D. W. Boeringer, and D. W. Machuga, "Optimization of thinned aperiodic linear phased arrays using genetic algorithms to reduce grating lobes during scanning," *IEEE Trans. Antennas Propagat.*, Vol. 50, No. 12, 1732–1742, Dec. 2002.
21. Bray, M. G., D. H. Werner, D. W. Boeringer, and D. W. Machuga, "Thinned aperiodic, linear phased array optimization for reduced grating lobes during scanning with input impedance bounds," *IEEE International Symposium on Antennas and Propagation Digest*, Vol. 3, 688–691, Boston, MA, July 2001.
22. Bossard, J. A., D. H. Werner, and M. G. Bray, "Efficient impedance interpolation and pattern approximation for linear microstrip phased arrays using neural networks," *USNC/URSI National Radio Science Meeting*, 102, Columbus, OH, June 2003.

23. DeLuccia, C. S. and D. H. Werner, "Nature-based design of aperiodic linear arrays with broadband elements using a combination of rapid neural network estimation techniques and genetic algorithms," *IEEE Antennas and Propagation Magazine*, Vol. 49, No. 5, 13–23, Oct. 2007.
24. Daniel, J. P., "Mutual coupling between antennas for emission or reception-application to passive and active dipoles," *IEEE Trans. Antennas Propagat.*, Vol. 22, No. 2, 347–349, 1973.
25. Taylor, T. T., "Design of line-source antennas for narrow beam width and low side lobes," *IRE Trans. Antenna Propagat.*, Vol. 3, 16–28, 1955.
26. FEKO 5.2, www.feko.info
27. Zhu, Y.-Z., Y.-J. Xie, Z.-Y. Lei, and T. Dang, "Array a novel method of mutual coupling matching for array antenna design," *J. of Electromagn. Waves and Appl.*, Vol. 21, No. 8, 1013–1024, 2007.
28. Zhou, Q., Y. J. Xie, and Z. Chen, "Prediction of equipment-to-equipment coupling through antennas mounted on an aircraft," *J. of Electromagn. Waves and Appl.*, Vol. 21, No. 5, 653–663, 2007.
29. Ayestaran, R. G., F. Las-Heras, and L. F. Herran, "High-accuracy neural-network-based array synthesis including element coupling," *IEEE Antennas and Wireless Propagation Letters*, Vol. 5, 45–48, 2006.
30. Mohamed, M. D. A., E. A. Soliman, and M. A. El-Gamal, "Optimization and characterization of electromagnetically coupled patch antennas using RBF neural networks," *J. of Electromagn. Waves and Appl.*, Vol. 20, No. 8, 1101–1114, 2006.
31. Guney, K., C. Yildiz, S. Kaya, and M. Turkmen, "Artificial neural networks for calculating the characteristic impedance of air-suspended trapezoidal and rectangular-shaped microshield lines," *J. of Electromagn. Waves and Appl.*, Vol. 20, No. 9, 1161–1174, 2006.
32. Ayestarán, R. G., J. Laviada, and F. Las-Heras, "Synthesis of passive-dipole arrays with a genetic-neural hybrid method," *J. of Electromagn. Waves and Appl.*, Vol. 20, No. 15, 2123–2135, 2006.
33. He, Q.-Q., "Conformal array based on pattern reconfigurable antenna and its artificial neural model," *J. of Electromagn. Waves and Appl.*, Vol. 22, No. 1, 99–110, 2008.